Horizontal Thrust in Vertically Curved Reinforced Concrete Beams

Ramakrishnan Subramanian, Ph.D.[1]; and Arun Murugesan, Ph.D., A.M.ASCE[2]

Abstract: This study was conducted to investigate the horizontal thrust of vertically curved reinforced concrete (VCRC) beams. The middle portion of beam is curved like an arch; such beams are said to be vertically curved beams. In this investigation, 15 VCRC beams were cast, of which, 8 beams had a constant rise of 200 mm and varying chord length of curved portion from 490 mm to 1832 mm, and the remaining 7 beams had a constant rise of 300 mm and varying chord length of curved portion from 690 mm to 1844 mm. The vertically curved portions of VCRC beams are in a parabolic shape. Tie bars were used to arrest longitudinal (horizontal) displacement while testing the VCRC beams. VCRC beams were subjected to a gradually increased central concentrated load until collapse occurred. The behavior of the beams was intensely observed from the beginning until collapse occurred. The first crack load, ultimate loads, deflection, and horizontal displacement have been recorded. The force in the tie bars was calculated based on the measured horizontal displacement. The total force in the tie bars is the available horizontal thrust at each end of a VCRC beam. Theoretical horizontal thrust of VCRC beams is calculated based on the force method. These theoretical thrust values and experimental results have been compared. The average value of the ratio of theoretical horizontal thrust to experimental horizontal thrust is found to be very satisfactory. **DOI: 10.1061/(ASCE)SC.1943-5576.0000418.**

Author keywords: Vertically curved reinforced concrete (VCRC) beam; Tie bars; Horizontal thrust; Chord length; Force method.

Introduction

Structural elements such as slabs, beams, lintel beams, columns, foundations, and arches are made of reinforced concrete (RC) because of its strength and durability. Various aspects of the history and development of the arch bridge have been discussed (Billington 1977). RC arches can be found in many structures, but they have been mainly used historically in bridge construction because of the superiority of the arch shape that allows spanning over large distances (Hamed et al. 2015). The arch is significant because it is predominantly subjected to compressive force while resisting the externally applied load. Utilizing the arch configuration in structural elements made with reinforced concrete has many advantages relating to the distance it can span and the loads it can carry. Nowadays, from an aesthetic point of view, arches are provided in combination with the straight portion of beams. This kind of combination of the straight portion and arch portion is named by the authors as vertically curved reinforced concrete (VCRC) beams. The authors attempt to study the behavior of VCRC beams is the first of its kind. The VCRC beams also transmit horizontal thrust due to the arch action of the curved portion. A significant interaction between shear, bending, and chord deviation forces occurs in arch-shaped RC members, influencing their strength and behavior (Campana et al. 2014b). In order to take care of horizontal thrust, tie bars were used in this investigation.

Research Significance

Godoy (2004) published an article titled *Arches: A Neglected Topic in Structural Analysis Courses*. This in-depth investigation highlights a deep rift between the modern level of development of arch theory and the level of presentation of this theory in existing material on structural analysis. Amde et al. (2002) reported on the stability tests of sandwich composite elastica arches. They investigated the novel sandwich elastica arch made by buckling its individual layers into shape, and then laminating them in place. Shankar Nair (1986) reported a method of computing the planar elastic buckling loads, natural frequencies, and corresponding mode shapes for arches and tied arches. The procedure involves linear elastic analysis with multiple loadings to obtain a simplified flexibility matrix, manual development of a stability matrix (for buckling) or mass matrix (for vibration), and solution of an eigenvalue equation.

Wang and Wang (2002) reformulated the differential equation in a coordinate system comprising the arc length and tangent angle and provided a solution that relates the arc length to the tangent angle of the arch for the determination of the submerged funicular arch. Chai and Kunnath (2003) reported that a closed-form solution for the shape of a submerged funicular arch is extended to Cartesian coordinates since it is more convenient from a practical design. RC arches subjected to bending or shear traditional design methods used for straight members were not applicable due to deviation forces developing at the curved chords carrying compression and tension, which were not always accounted in design codes (Campana et al. 2014a).

The main objective of this investigation is to develop a method to predict the horizontal thrust at hinged supports when VCRC beams are subjected to a gradually increased central concentrated

[1]Associate Professor, Dept. of Civil Engineering, Bannari Amman Institute of Technology, Sathyamangalam 638401, India (corresponding author). Email: ramakrishnans@bitsathy.ac.in

[2]Assistant Professor, Dept. of Civil Engineering, PSG Institute of Technology and Applied Research, Coimbatore 641062, India. Email: arun@psgitech.ac.in

Note. This manuscript was submitted on July 24, 2018; approved on December 7, 2018; published online on January 30, 2019. Discussion period open until June 30, 2019; separate discussions must be submitted for individual papers. This paper is part of the ***Practice Periodical on Structural Design and Construction***, © ASCE, ISSN 1084-0680.

load. Sufficient methods are available for the analysis of arches. Fixed arches are more commonly encountered than hinged arches because all masonry arches are considered fixed arches. In order to analyze these kinds of arches, the well-known analysis methods, such as Castigliano's, elastic center, or column analogy, can be conveniently adopted. However, there are no theories or literature available to predict the horizontal thrust of VCRC beams. Hence, an experimental and theoretical investigation was originated.

Experimental Investigation

Vertically Curved Reinforced Concrete Beam Details

Fifteen parabolic VCRC beams with a rectangular cross section width of 200 mm, depth of 150 mm, and effective span of 1,900 mm were cast and tested. Out of these, eight beams were cast with a constant rise of 200 mm, and the remaining seven beams were cast with a constant rise of 300 mm. The rise (r), length of the straight portion on one side (L_1), chord length of the curved portion (L_2), and beam designations of VCRC beams are given in Table 1. The rise-to-span ratio of the arch was chosen to fall within a range of typical values reported from existing RC arches (Billington 1979; Dym and Williams 2011; Salonga and Gauvreau 2014). The high yield strength deformed (HYSD) bars were used as reinforcement bars. All VCRC beams consisted of the same reinforcement. Details are presented in Fig. 1.

Fabrication of Molds and Casting of Vertically Curved Reinforced Concrete Beams

All VCRC beams were combinations of parabolically curved and straight portions. The mold preparation for the curved portion was cumbersome; initially, coordinates of curves were determined for the parabolic curved portion. The equation of the parabolic line of the curved portion is

$$y = \frac{4rx}{L_2{}^2}(L_2 - x) \tag{1}$$

where L_2 = chord length; r = central rise; and $y_1, y_2, \ldots$ = vertical coordinates corresponding to the horizontal coordinates $x_1, x_2, \ldots$, respectively. From Eq. (1), the various coordinate points, $y_1, y_2, \ldots$, were calculated, and ordinates were erected on the base line corresponding to $x_1, x_2, \ldots$, respectively, as presented in Fig. 2.

The coordinate points corresponding to the center line of the curved portion were plotted on a horizontal base plate, and with respect to this center line, flexible plywood pieces were fixed defining the inner and outer sides of the curved portion. The fabricated mold of VCRC beams is presented in Fig. 3. To maintain the homogeneity of concrete, all the beams were cast horizontally and tested vertically (Ramakrishnan 2015). The reinforcement was placed inside the mold on cover blocks of size 20 mm. The M20 grade concrete has been mixed in a concrete mixer, put inside the mold in three layers, and compacted well using a needle vibrator. Twenty-four hours after casting, the beams were demolded, and the VCRC beams were cured under wet gunny bags for 28 days. The gunny

Table 1. Experimental results of VCRC beams

Serial number	Beam	r (mm)	L_1 (mm)	L_2 (mm)	L_2:L	$(W_{cr})_E$ (kN)	$(W_u)_E$ (kN)	Central deflection (mm)	δ_t (mm)	H_E (kN)
1	$PP_0C_{400}H$	200	705	490	0.258	16	44	1.034	0.97	154.102
2	$PP_0C_{600}H$	200	614	672	0.354	18	58	0.754	1.23	194.244
3	$PP_0C_{800}H$	200	520	860	0.453	20	70	0.568	1.50	237.580
4	$PP_0C_{1000}H$	200	424	1,052	0.554	24	88	0.438	2.03	320.791
5	$PP_0C_{1200}H$	200	328	1,244	0.655	26	96	0.372	2.45	388.199
6	$PP_0C_{1400}H$	200	230	1,440	0.758	30	106	0.306	2.61	412.550
7	$PP_0C_{1600}H$	200	133	1,634	0.860	32	114	0.255	2.82	446.729
8	$PP_0C_{1800}H$	200	34	1,832	0.964	34	128	0.21	3.11	493.037
9	$PP_1C_{600}H$	300	605	690	0.363	20	64	0.602	1.05	166.643
10	$PP_1C_{800}H$	300	511	878	0.462	24	86	0.503	1.37	216.323
11	$PP_1C_{1000}H$	300	416	1,068	0.562	28	106	0.393	1.73	274.515
12	$PP_1C_{1200}H$	300	320	1,260	0.663	32	120	0.334	2.08	329.969
13	$PP_1C_{1400}H$	300	223	1,454	0.765	36	138	0.259	2.45	388.090
14	$PP_1C_{1600}H$	300	125	1,650	0.868	40	156	0.206	2.78	440.898
15	$PP_1C_{1800}H$	300	28	1,844	0.971	46	174	0.189	3.09	488.430

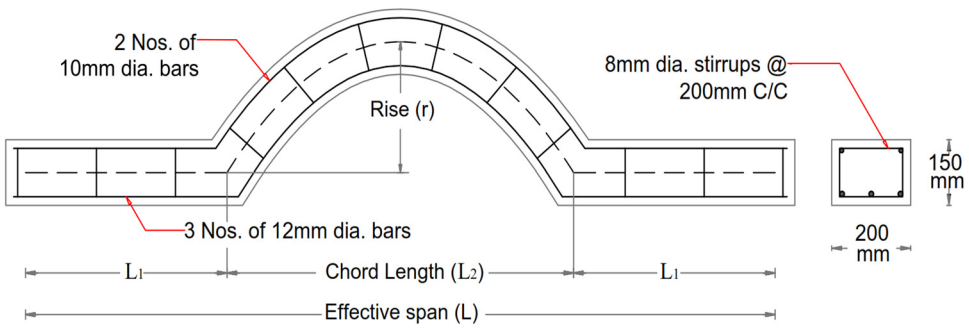

Fig. 1. Reinforcement details for VCRC beam.

Pract. Period. Struct. Des. Constr., 2019, 24(2): 04019005

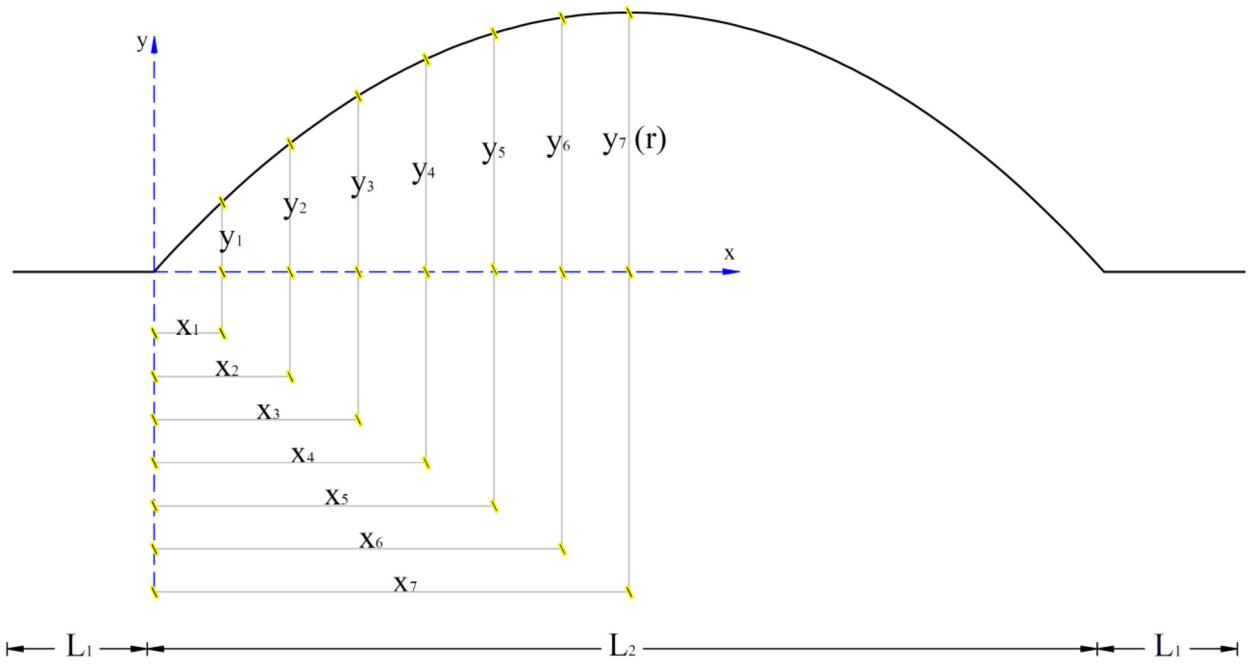

Fig. 2. Coordinate points for VCRC beam.

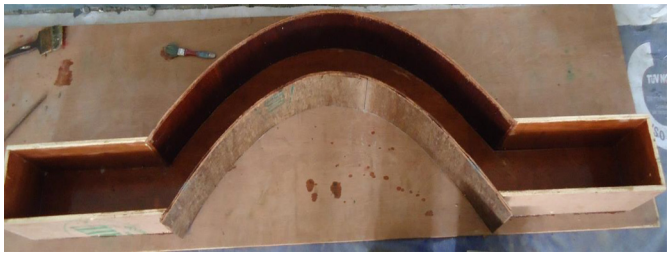

Fig. 3. Fabricated mold for VCRC beam.

bags were watered thrice a day, taking special care to see that all the parts were watered uniformly.

Loading Setup of Vertically Curved Reinforced Concrete Beams

All the VCRC beams were tested with tie bars to minimize the longitudinal displacement and to promote the arch action in the curved portion. Initially, VCRC beams were placed over the steel support with 100-mm bearings on both ends of the beam. The two mild steel rods 32 mm in diameter were used as tie bars; the ends of these rods were threaded. The steel plates of 16 mm thickness were placed at the beam ends, these plates having two holes 34 mm in diameter to accommodate the tie bars. Tie bars were also passed through the holes provided in the steel plates. Tightening the four nuts on each of the tie bars and fastening the two tie bars with steel plates at the ends of the beam ensured that the longitudinal displacement of VCRC beams was arrested. All the VCRC beams were tested up to failure in a steel self-straining loading frame of capacity 750 kN (Murugesan and Narayanan 2017, 2018). The gradually increased central concentrated load was applied using a hydraulic jack in increments of 2 kN until collapse of the beam occurred, and it was measured using a calibrated proving ring. Horizontal displacements were measured by means of one dial gauge fixed at each end of a VCRC beam. Deflections of beams were measured by linear

Fig. 4. Testing arrangements of VCRC beam with tie bars.

variable differential transducer (LVDT) at L/8, L/4, and L/2 from each support. A test setup of VCRC beams is presented in Fig. 4.

Results of Experimentation

Strength and Deflection of Vertically Curved Reinforced Concrete Beams

The ratio of chord length (L_2) to effective span (L) varied from 0.258 to 0.964 for a 200-mm rise and from 0.363 to 0.971 for 300-mm rise. The first crack load, ultimate load, precrack central deflections corresponding to the load of 8 kN, horizontal displacement, and horizontal thrust (force in the tie bars) of VCRC beams are given in Table 1.

The first crack load and ultimate load-carrying capacity of VCRC beams were found to increase as the L_2:L increased, because there was more contribution by the arch action of the vertically curved portion. The load-carrying capacity of beams increased with

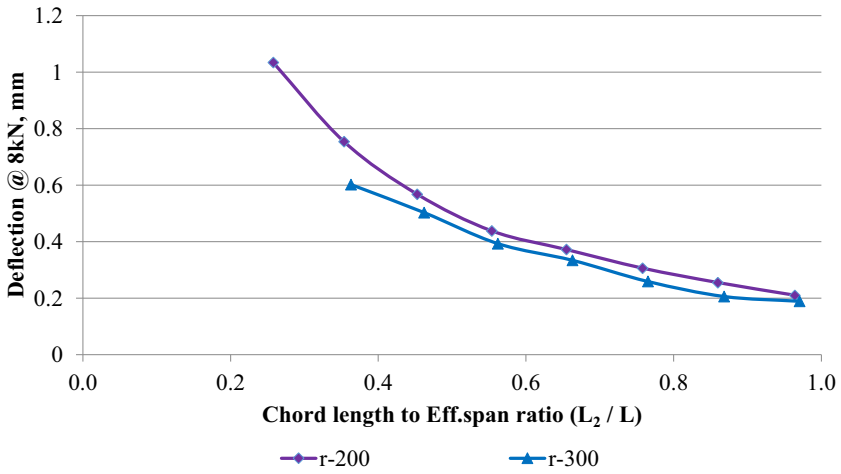

Fig. 5. Central deflections for various L_2:L ratios under 8 kN load.

the increase in the rise of the curved portion of VCRC beams. This can be attributed to the increase in arch action with a higher rise (Ramakrishnan and Arunachalam 2016). The variation of central deflection with L_2:L in VCRC beams is shown in Fig. 5. The central vertical deflection of VCRC beams decreased as the ratio of L_2:L increased because the vertical load transmitted by the curved portion to the straight portion was closer to the supports. In addition, for a given L_2:L, the central deflection decreases as the rise increases.

Crack Pattern of Vertically Curved Reinforced Concrete Beams

The tested VCRC beams had the L_2:L ratio less than 0.453, and flexural cracks developed initially on either side of the junctions between the straight portion and curved portion. When the load was increased, these cracks widened. Finally, the beams failed due to the formation of horizontal cracks in the curved portion at the ultimate load. The beams that had the L_2:L ratio greater than 0.453 failed due to vertical cracks that appeared in the curved portion, and very thin horizontal cracks were seen in the curved portion. These beams failed due to the widening of vertical cracks, because the spreading of the curved portion had been arrested by tie bars to a greater extent. The crack patterns of 200 mm and 300 mm rise in VCRC beams are presented in Figs. 6 and 7.

Horizontal Thrust in Vertically Curved Reinforced Concrete Beams

A VCRC beam transmits horizontal force at the ends because of the arch action by the curved portion. In order to prevent this horizontal force, two tie bars with threaded ends were placed symmetrically, one on each side of the beam, and anchored at the ends using nuts. The sum of the displacements measured at the ends of beams was the axial deformation in the two tie bars. Based on this, the horizontal force in the two tie bars was calculated. The horizontal force in the two tie bars is equal to the horizontal thrust at each end of the VCRC beam. The horizontal force in the tie bars is

$$H_E = \frac{\delta_t A_t E_t}{L_t} \tag{2}$$

where δ_t = elongation of the tie bars, which is equal to the sum of the measured displacements of the two ends of beams; A_t = total area of the cross section of tie bars of 1608.49 mm^2 (2 numbers of 32 mm diameter); E_t = Young's modulus of the materials of the tie bars 2×10^5 N/mm^2; and L_t = length of tie bars (length of beam plus twice the thickness of one end plate) 2,032 mm. The experiment horizontal thrust values at the ultimate load for VCRC beams are listed in Table 1.

Theoretical Calculation for Horizontal Thrust

Theoretical calculation for the horizontal thrust of VCRC beams is based on the force method. The force method is very attractive because it has a clear physical meaning, which is based on a convenient and well-ordered procedure of calculation of displacements of deformable structures, and presently, this method has been brought to elegant simplicity and perfection (Karnovsky 2012). Primary unknowns represent reactions (forces and/or moments), which arise in redundant constraints. Unknown internal forces also may be treated as primary unknowns. The primary system is such a structure, which is obtained from the given one by eliminating redundant constraints and replacing them by primary unknowns. Let the primary unknown X_1 be the horizontal reaction of the right support. The primary system is given in Fig. 8(a); this structure is subjected to given loads as well as the force X_1.

The equation of the force method is

$$\delta_{11} X_1 + \Delta_{1p} = 0$$

$$\therefore X_1 = \frac{-\Delta_{1p}}{\delta_{11}} \tag{3}$$

where δ_{11} = coefficient that represents the displacement of the primary structure along the direction of unknown X_1 due to the unit primary unknown given in Fig. 8(b). This displacement is always positive, that is, $\delta_{11} > 0$. The term $\delta_{11} X_1$ represents the displacement along the direction of unknown X_1 due to the action of the real unknown X_1. The free term Δ_{1p} represents displacement in the primary system along the direction of unknown X_1 due to the action of the actual load. Displacement caused by applied loads Δ_{1p} is called load term, as presented in Fig. 8(c). The left part, $\delta_{11} X_1 + \Delta_{1p}$, represents the total displacement along the direction of unknown X_1 due to its action and a given load. Total displacement, which occurs in the primary structure, is caused by the primary unknown, and the applied load equals zero (Karnovsky and Lebed 2004, 2010). A VCRC beam with tie bars is a structure with one redundant constraint. The internal force in tie bars may be treated as the primary unknown X_1. In this

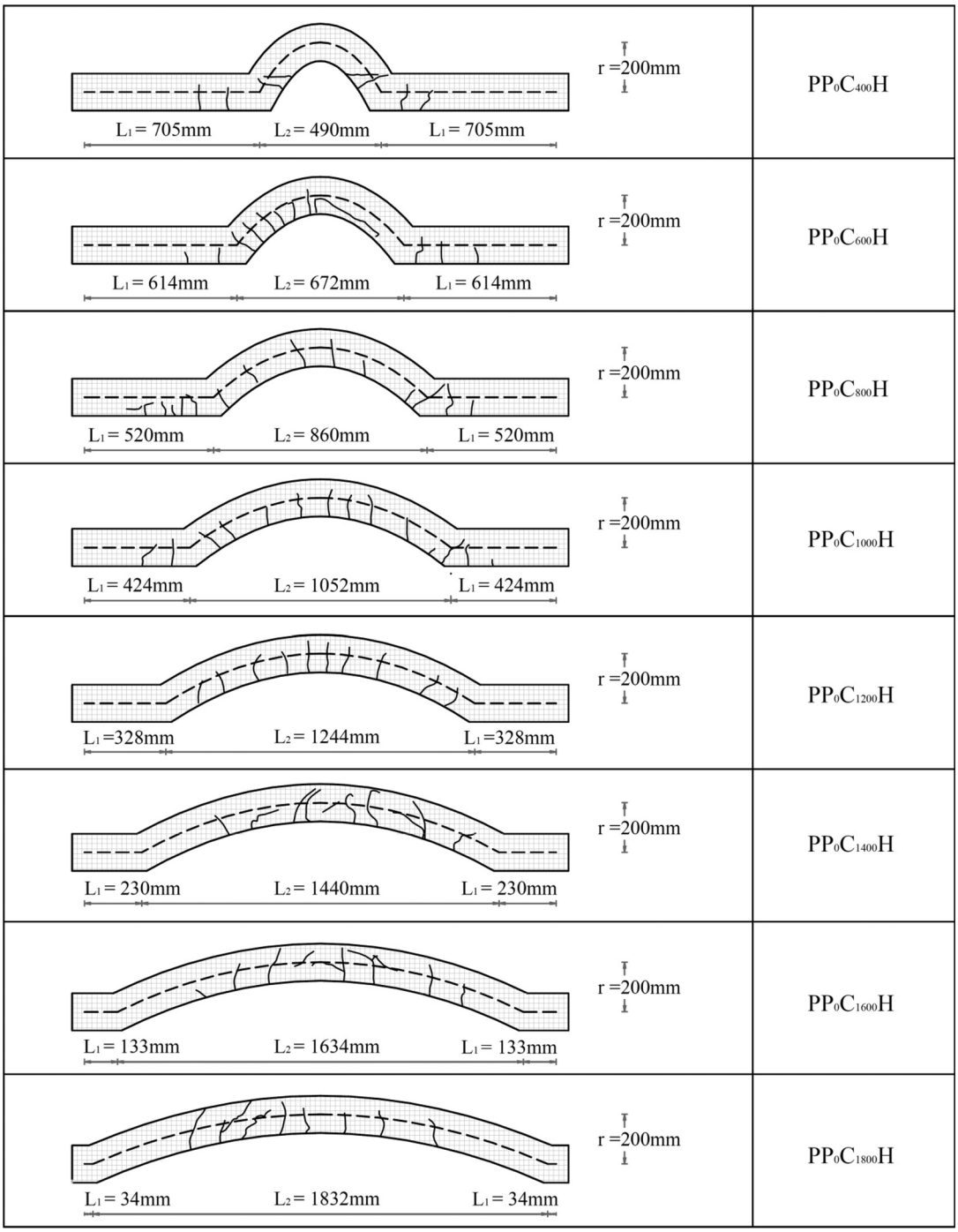

Fig. 6. Crack pattern of 200-mm rise VCRC beams.

case, the primary system represents a simply supported curvilinear rod. The coefficient δ_{11} is a mutual linear displacement due to the unit force $X_1 = 1$, and Δ_{1p} is a mutual linear displacement in the tie due to the given load. The equation means that the mutual linear displacement of any two sections, which belongs to the tie, caused by primary unknown X_1 and a given load, is equal to zero.

Modal Calculation for Horizontal Thrust in a Vertically Curved Reinforced Concrete Beam

The ends of a VCRC beam are assumed to be hinged, because the horizontal thrusts are developed by tie rods. For analysis of VCRC beams, the shape of the beam is converted into equivalent arches with an end moment ($M_s = WL_{1/2}$). Consider the beam $PP_1C_{1000}H$ presented in Fig. 9(a). The forces and moments acting on the curved portion of a VCRC beam are presented in Fig. 9(b). The flexural stiffness of the cross section of the curved portion is EI. The equation of the parabolic line of the curved portion is given in Eq. (1).

It is necessary to find the distribution of internal forces. The curved portion under investigation is statically indeterminate to the first degree. The primary system is presented in Fig. 9(d). The primary unknown X_1 is the horizontal reaction of the right support. Let us subdivide the arch into segments with equal horizontal projections. The span of the curved portion is divided into ten equal parts; the specified points are labeled 0–10 as given in Fig. 9(c).

Pract. Period. Struct. Des. Constr., 2019, 24(2): 04019005

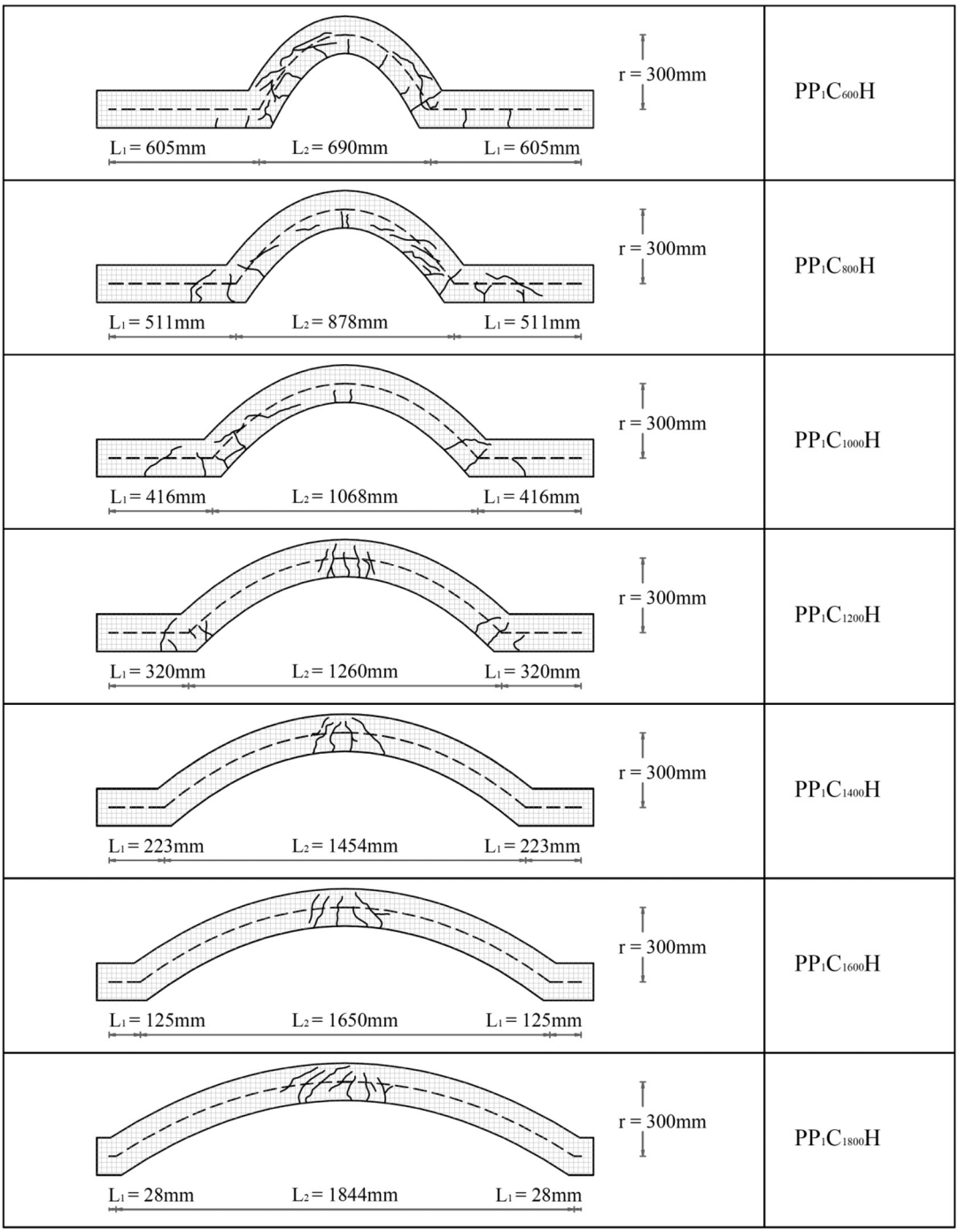

Fig. 7. Crack pattern of 300-mm rise VCRC beams.

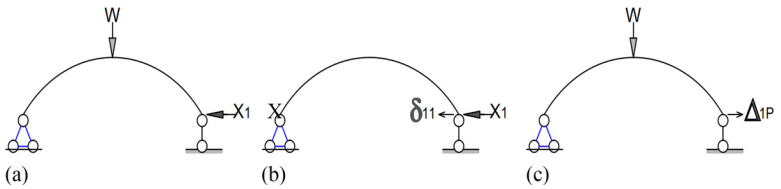

Fig. 8. Application of the force method: (a) primary system; (b) primary system with unit load; and (c) displacement due to applied load.

Pract. Period. Struct. Des. Constr., 2019, 24(2): 04019005

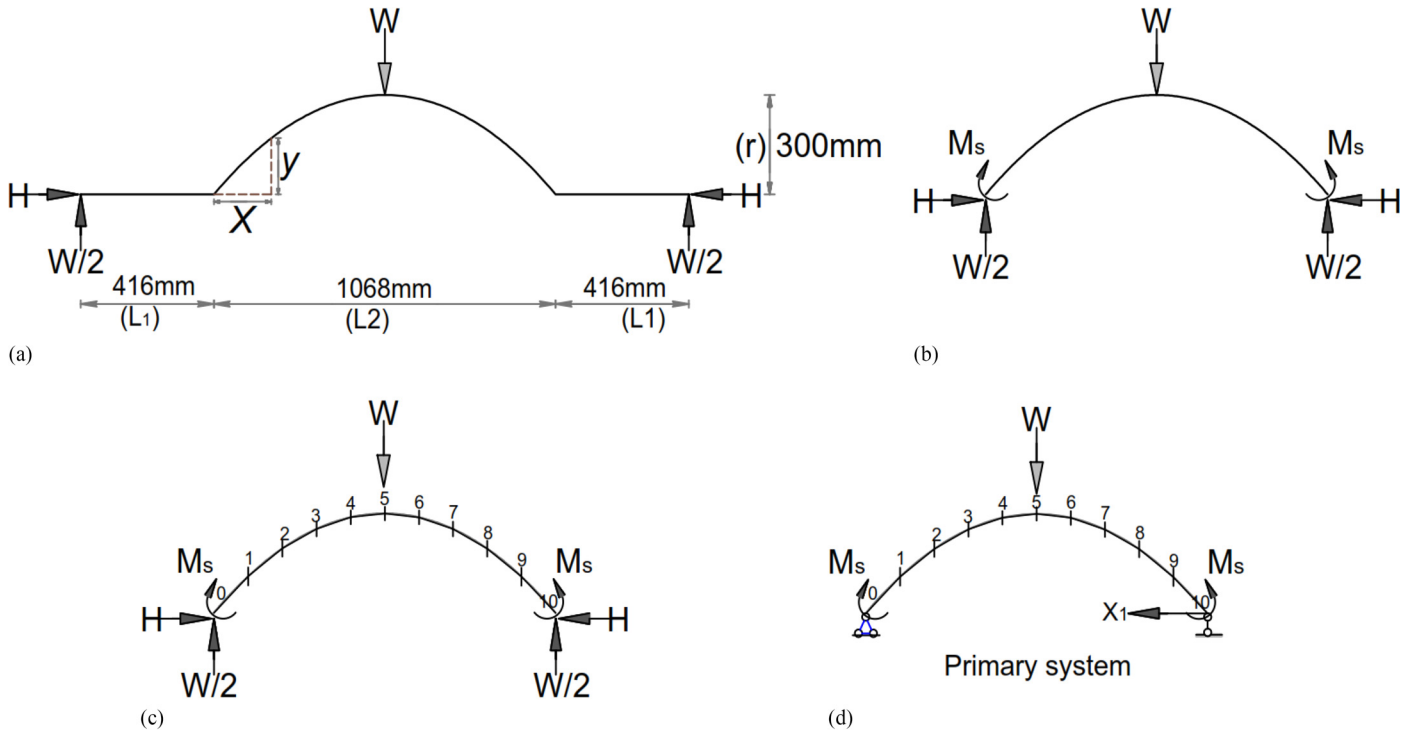

Fig. 9. Primary system of $PP_1C_{1000}H$ beam: (a) VCRC beam $PP_1C_{1000}H$; (b) forces in curved portion; (c) segments of curved portion; and (d) primary system of $PP_1C_{1000}H$.

Table 2. Internal forces due to the unit and loaded states of beam $PP_1C_{1000}H$

	Coordinates					Unit state ($H = 1$)			Loaded state in terms of W		
Points	x (mm)	y (mm)	$\tan\phi$	$\cos\phi$	$\sin\phi$	M_1 (kN·mm)	Q_1 (kN)	N_1 (kN)	M_p (kN·mm)	Q_p (kN)	N_p (kN)
0	0	0	1.12	0.67	0.75	0	−0.75	−0.67	208	0.33	−0.37
1	107	108	0.90	0.74	0.67	−108	−0.67	−0.74	261.4	0.37	−0.33
2	214	192	0.67	0.83	0.56	−192	−0.56	−0.83	314.8	0.42	−0.28
3	320	252	0.45	0.91	0.41	−252	−0.41	−0.91	368.2	0.46	−0.21
4	427	288	0.23	0.98	0.22	−288	−0.22	−0.98	421.6	0.49	−0.11
5	534	300	0.00	1.00	0.00	−300	0.00	−1.00	475	0.50	0.00
6	641	288	−0.23	0.98	−0.22	−288	0.22	−0.98	528.4	0.49	0.11
7	748	252	−0.45	0.91	−0.41	−252	0.41	−0.91	581.8	0.46	0.21
8	854	192	−0.67	0.83	−0.56	−192	0.56	−0.83	961.2	0.42	0.28
9	961	108	−0.90	0.74	−0.67	−108	0.67	−0.74	688.6	0.37	0.33
10	1,068	0	−1.12	0.67	−0.75	0	0.75	−0.67	742	0.33	0.37

The following formulas for the calculation of trigonometric functions of the angle between the tangent to the curved portion and x-axis have been used. Results of the calculations are presented in Table 2.

$$\tan\varphi = \frac{dy}{dx} = \frac{4r(L_2 - 2x)}{L_2^2}; \quad \cos\varphi = \frac{1}{\sqrt{1 + \tan^2\varphi}};$$
$$\sin\varphi = \cos\varphi \tan\varphi \tag{4}$$

The length of the chord (l_c) between points is calculated using the following formula for all segments of beam $PP_1C_{1000}H$.

$$l_{cn,n-1} = \sqrt{(x_n - x_{n-1})^2 + (y_n - y_{n-1})^2} \tag{5}$$

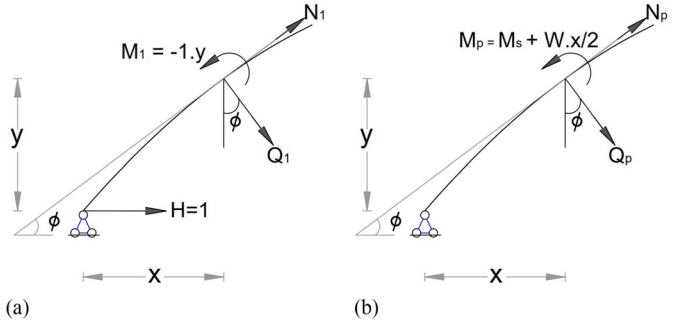

Fig. 10. Positive directions of internal forces in the (a) unit state; and (b) loaded state.

Table 3. The moment values for each element

Portion	l_c (mm)	Unit state ($H = 1$)				Loaded state in terms of W			
		a_1	c_1	b_1	$(l_c/6)\cdot(a_1^2 + 4c_1^2 + b_1^2)$	a_p	c_p	b_p	$(l_c/6)\cdot(a_1a_p + 4c_1c_p + b_1b_p)$
(0–1)	151.89	0	−54	−108	590,544.07	208.0	234.7	261.4	−1,998,007.44
(1–2)	135.88	−108	−150	−192	3,137,101.06	261.4	288.1	314.8	−5,922,664.19
(2–3)	122.50	−192	−222	−252	6,074,037.98	314.8	341.5	368.2	−9,319,796.89
(3–4)	112.70	−252	−270	−288	8,228,309.30	368.2	394.9	421.6	−12,034,916.69
(4–5)	107.47	−288	−294	−300	9,290,743.16	421.6	448.3	475.0	−14,170,575.75
(5–6)	107.47	−300	−294	−288	9,290,743.16	475.0	501.7	528.4	−15,846,365.82
(6–7)	112.70	−288	−270	−252	8,228,309.30	528.4	555.1	581.8	−16,873,714.36
(7–8)	122.50	−252	−222	−192	6,074,037.98	581.8	771.5	961.2	−20,748,553.09
(8–9)	135.88	−192	−150	−108	3,137,101.06	961.2	824.9	688.6	−17,071,873.54
(9–10)	151.89	−108	−54	0	590,544.07	688.6	715.3	742.0	−5,793,893.48
Total					54,641,471.15				−119,780,361.26

Table 4. Comparison of horizontal thrust values of VCRC beams at ultimate loads

Beam	r (mm)	W_u (kN)	Theoretical thrust in terms of W_u (kN)	Theoretical thrust [H_T (kN)]	Experimental thrust [H_E (kN)]	H_T:H_E
$PP_0C_{400}H$	200	44	3.196	140.624	154.102	0.913
$PP_0C_{600}H$	200	58	3.106	180.148	194.244	0.927
$PP_0C_{800}H$	200	70	3.058	214.060	237.580	0.901
$PP_0C_{1000}H$	200	88	3.230	284.240	320.791	0.886
$PP_0C_{1200}H$	200	96	3.328	319.488	388.199	0.823
$PP_0C_{1400}H$	200	106	3.385	358.810	412.550	0.870
$PP_0C_{1600}H$	200	114	3.421	389.994	446.729	0.873
$PP_0C_{1800}H$	200	128	3.432	439.296	493.037	0.891
$PP_1C_{600}H$	300	64	2.112	135.168	166.643	0.811
$PP_1C_{800}H$	300	86	2.072	178.192	216.323	0.824
$PP_1C_{1000}H$	300	106	2.192	232.352	274.515	0.846
$PP_1C_{1200}H$	300	120	2.242	269.040	329.969	0.815
$PP_1C_{1400}H$	300	138	2.271	313.398	388.090	0.808
$PP_1C_{1600}H$	300	156	2.291	357.396	440.898	0.811
$PP_1C_{1800}H$	300	174	2.343	407.682	488.430	0.835
Average	—	—	—	—	—	0.856
Standard deviation	—	—	—	—	—	0.041
Coefficient of variation	—	—	—	—	—	4.800

Internal Forces in the Unit State

The curved portion is subjected to unit primary unknown $X_1 = 1$. The horizontal reaction $H = 1$ and the positive directions of internal forces of moment (M_1), shear (Q_1), and axial force (N_1) are given in Fig. 10(a). Internal forces at all the segmental points are listed in Table 2.

$$M_1 = -1y; \quad Q_1 = -1\sin\varphi; \quad N_1 = -1\cos\varphi \tag{6}$$

Internal Forces in the Loaded State

Due to the applied load, W, the positive directions of internal stress resultants of moment (M_p), shear (Q_p), and axial force (N_p) are given in Fig. 10(b). They were calculated using the following expressions. Internal forces at all the segmental points due to the loaded state are listed in Table 2.

$$M_p = M_s + \frac{Wx}{2}; \quad Q_p = \frac{W\cos\varphi}{2}; \quad N_p = \frac{-W\sin\varphi}{2} \tag{7}$$

The displacements due to unit load and loaded terms are calculated by Maxwell-Mohr formulas. If the shear and axial force are neglected, because they are very small, then the Simpson formula is applied for the calculation of displacement. The displacement due to unit load (δ_{11}) caused by primary unknown $X = 1$ equals

$$\delta_{11} = \int \frac{M_1M_1}{EI}\,ds = \sum_1^{10} \frac{l_c}{6EI}\left(a_1^2 + 4c_1^2 + b_1^2\right) = \frac{54641471.15}{EI} \tag{8}$$

Displacement in the primary system (Δ_{1p}) caused by the applied load is given by

$$\Delta_{1P} = \int \frac{M_1M_P}{EI}\,ds = \sum_1^{10} \frac{l_c}{6EI}\left(a_1a_p + 4c_1c_p + b_1b_p\right) = \frac{-119780361.26\ W}{EI} \tag{9}$$

where $M_p = M_s + \mathrm{W}$; x / 2 = bending moments at any point of the curved portion in the loaded state; a_1, a_p = ordinates of the bending moment diagrams M_1 and M_p at the extreme left end of the portion; b_1, b_p = ordinates of the same bending moment diagrams at the

extreme right end of the portion; and c_1, c_p = ordinates of the same bending moment diagrams at the middle point of the portion. The moment values of each element are given in Table 3.

The primary unknown (thrust) become $X_1 = -\Delta_{1p}/\delta_{11} = 2.192\,W$. Therefore, the theoretical horizontal thrust of $PP_1C_{1000}H$ beams is $(H_t) = 2.192\,W$. Similarly, for all VCRC beams, the theoretical horizontal thrusts have been calculated and are given in Table 4. Theoretical thrust values are in terms of applied load, W. The force method, even though developed for elastic analysis, is applied to predict the horizontal thrust at the ends of VCRC beams when the beams carry the ultimate load.

Comparison of Horizontal Thrust Values of Vertically Curved Reinforced Concrete Beams

The theoretical horizontal thrust available at the ends of VCRC beams corresponding to the hinged condition of the ends and experimental horizontal thrust provided by the tie bars at the ends of beams are compared in Table 4. The average value of the ratio of theoretical horizontal thrust to experimental horizontal thrust is found to be 0.856 with standard deviation of 0.041 and coefficient of variation 4.8%. This shows that in the case of VCRC beams, the horizontal displacement at the ends of the beams is prevented, and the horizontal thrust experienced by the beams at the ultimate load can satisfactorily be calculated using the force method of analysis.

Conclusions

In order to study the horizontal thrust, strength, and behavior of VCRC beams, a total of 15 VCRC beams were cast. Out of these, 8 beams had a constant rise of 200 mm, and 7 beams had a constant rise of 300 mm. All the VCRC beams were of the same span and cross section. All the beams were tested with tie bars subjected to a gradually increased central concentrated load until failure occurred. The horizontal thrust, strength, and behavior were recorded. The theoretical analysis of the horizontal thrust of VCRC beams was calculated based on the force method. Based on experimentation and theoretical analysis, the following conclusion are drawn:

1. It is observed that as the chord length (L_2) increases, the first crack load and ultimate load-carrying capacity of VCRC beams increases because of a greater arch action promoted by the curved portion of the beam.
2. For a given L_2:L ratio, the first crack load and ultimate load of VCRC beams increases as the rise of the curved portion increases. This can be attributed to the increase in arch action with higher rise.
3. The central deflection decreases as the chord length L_2 increases. This can be attributed to the fact that the greater the chord length, the greater the arch action, due to the availability of greater horizontal thrust offered by tie bars resulting in the reduction of central deflection.
4. For a given L_2:L ratio, the deflection of VCRC beams decreases as the rise of the curved portion increases. This can be attributed to the increase in arch action with a higher rise.
5. In an L_2:L ratio less than 0.453, the flexural cracks developed initially on either side of the junctions. The beams failed due to the formation of horizontal cracks in the curved portion at the ultimate load.
6. The beams that had the L_2:L ratio greater than 0.453 failed due to vertical cracks and very thin horizontal cracks that appeared in the curved portion. These beams failed due to the widening of the vertical cracks, because spreading of the curved portion had been arrested by tie bars to a greater extent.
7. A VCRC beam with hinged support transmits a horizontal force at the two ends because of the arch action by the curved portion. In order to simulate the hinged supports, two tie bars, one on each side of the beam and anchored at the ends, were adopted. The sum of the displacements measured at the ends of the beams was the axial deformation in the two tie bars. Based on this, the horizontal force in the two tie bars was calculated. The horizontal force in the two tie bars is equal to the horizontal thrust at each end of a VCRC beam.
8. Using the force method of analysis, a process is suggested to predict the horizontal thrust in VCRC beams at the ultimate load whenever the ends are prevented from moving horizontally.
9. The average value of the ratio of theoretical horizontal thrust obtained by this equation to experimental horizontal thrust is found to be 0.856 with a standard deviation of 0.041 and a coefficient of variation of 4.8%. This shows that when the horizontal displacements at ends of the beams are prevented, the horizontal thrust experienced by the VCRC beams at the ultimate load can satisfactorily be predicted using the force method of analysis.

Acknowledgments

The experimental investigation was carried out at the Concrete and Structural Engineering Research Laboratory, Department of Civil Engineering, Bannari Amman Institute of Technology, Sathyamangalam, India. The authors would like to thank Dr. Arunachalam Narayanan, former professor, PSG College of Technology, who was a technical advisor for this work, and thanks to all the staff members of the Civil Engineering Department and technicians of the laboratory for their helpful assistance in the preparation and testing of beams.

Notation

The following symbols are used in this paper:

a_1 = ordinate of the bending moment for the unit state at the left end of a segment of the curved portion;
a_p = ordinate of the bending moment for the loaded state at the left end of a segment of the curved portion;
A_{st} = area of tensile steel;
b_1 = ordinate of the bending moment for the unit state at the right end of a segment of the curved portion;
b_p = ordinate of the bending moment for the loaded state at the right end of a segment of the curved portion;
c_1 = ordinate of the bending moment for the unit state at the middle point of a segment of the curved portion;
c_p = ordinate of the bending moment for the loaded state at the middle point of a segment of the curved portion;
$(H)_E$ = experimental horizontal thrust of a VCRC beam;
$(H)_T$ = theoretical horizontal thrust of a VCRC beam;
L = effective span;
L_1 = length of the straight portion of the VCRC beam on one side of the curved portion;
L_2 = chord length of the curved portion of the VCRC beam;
L_2:L = chord length to effective span ratio;

l_c = length of chord between adjacent points in the curved portion;
L_t = length of tie bars;
LVDT = linear variable differential transducer;
M_1 = moment at the unit state;
M_{cr} = midspan bending moment of beam at the first crack load;
M_p = moment at the loaded state;
N_1 = axial force at the unit state;
N_p = axial force at the loaded state;
$PP_0C_{400}H$ = VCRC beam of rise 200 mm and inner chord length 400 mm;
$PP_0C_{600}H$ = VCRC beam of rise 200 mm and inner chord length 600 mm;
$PP_0C_{800}H$ = VCRC beam of rise 200 mm and inner chord length 800 mm;
$PP_0C_{1000}H$ = VCRC beam of rise 200 mm and inner chord length 1000 mm;
$PP_0C_{1200}H$ = VCRC beam of rise 200 mm and inner chord length 1200 mm;
$PP_0C_{1400}H$ = VCRC beam of rise 200 mm and inner chord length 1400 mm;
$PP_0C_{1600}H$ = VCRC beam of rise 200 mm and inner chord length 1600 mm;
$PP_0C_{1800}H$ = VCRC beam of rise 200 mm and inner chord length 1800 mm;
$PP_1C_{600}H$ = VCRC beam of rise 300 mm and inner chord length 600 mm;
$PP_1C_{800}H$ = VCRC beam of rise 300 mm and inner chord length 800 mm;
$PP_1C_{1000}H$ = VCRC beam of rise 300 mm and inner chord length 1000 mm;
$PP_1C_{1200}H$ = VCRC beam of rise 300 mm and inner chord length 1200 mm;
$PP_1C_{1400}H$ = VCRC beam of rise 300 mm and inner chord length 1400 mm;
$PP_1C_{1600}H$ = VCRC beam of rise 300 mm and inner chord length 1600 mm;
$PP_1C_{1800}H$ = VCRC beam of rise 300 mm and inner chord length 1800 mm;
Q_1 = shear at the unit state;
Q_p = shear at the loaded state;
r = rise of the VCRC beam;
W_{cr} = first crack load of the VCRC beam;
W_u = ultimate load of the VCRC beam;
Δ_{1p} = displacement in the primary system for the loaded state;
δ_{11} = displacement in the primary system for the unit state; and
δ_t = elongation of the tie bars.

References

Amde, A. M., A. Mirmiran, and D. Nelsen. 2002. "Stability tests of sandwich composite elastica arches." *J. Struct. Eng.* 128 (5): 683–686. https://doi.org/10.1061/(ASCE)0733-9445(2002)128:5(683).

Billington, D. P. 1977. "History and esthetics in concrete arch bridges." *J. Struct. Div.* 103 (11): 2129–2143.

Billington, D. P. 1979. *Robert Maillart's bridges: Art of engineering.* Princeton, NJ: Princeton University Press.

Campana, S., M. Fernández Ruiz, and A. Muttoni. 2014a. "Strength of arch-shaped members in bending and shear." In *Proc., 4th fib Congress*, 9–18. Mumbai, India: Structural Concrete Laboratory of EPFL.

Campana, S., M. Fernandez Ruiz, and A. Muttoni. 2014b. "Shear strength of arch-shaped members without transverse reinforcement." *ACI Struct. J.* 111 (3): 573–582.

Chai, Y., and S. Kunnath. 2003. "Geometry of submerged funicular arches in Cartesian coordinates." *J. Struct. Eng.* 129 (8): 1087–1092. https://doi.org/10.1061/(ASCE)0733-9445(2003)129:8(1087).

Dym, C. L., and H. E. Williams. 2011. "Stress and displacement estimates for arches." *J. Struct. Eng.* 137 (1): 49–58. https://doi.org/10.1061/(ASCE)ST.1943-541X.0000267.

Godoy, L. A. 2004. "Arches: A neglected topic in structural analysis courses." In *Proc., ASEE Southeastern Section Conf.*, Auburn, AL: ASEE.

Hamed, E., Z.-T. Chang, and O. Rabinovitch. 2015. "Strengthening of reinforced concrete arches with externally bonded composite materials: Testing and analysis." *J. Compos. Constr.* 19 (1): 04014031. https://doi.org/10.1061/(ASCE)CC.1943-5614.0000495.

Karnovsky, I. A. 2012. *Theory of arched structures.* New York: Springer.

Karnovsky, I. A., and O. Lebed. 2004. *Non-classical vibrations of arch and beams: Eigenvalues and eigenfunctions.* New York: McGraw-Hill.

Karnovsky, I. A., and O. Lebed. 2010. *Advanced methods of structural analysis.* New York: Springer.

Murugesan, A., and A. Narayanan. 2017. "Influence of a longitudinal circular hole on flexural strength of reinforced concrete beams." *Pract. Period. Struct. Des. Constr.* 22 (2): 04016021. https://doi.org/10.1061/(ASCE)SC.1943-5576.0000307.

Murugesan, A., and A. Narayanan. 2018. "Deflection of reinforced concrete beams with longitudinal circular hole." *Pract. Period. Struct. Des. Constr.* 23 (1): 04017034. https://doi.org/10.1061/(ASCE)SC.1943-5576.0000356.

Ramakrishnan, S. 2015. "Behavior and strength of reinforced concrete beams partly curved in elevation." Ph.D. thesis, Dept. of Civil Engineering, Bannari Amman Institute of Technology.

Ramakrishnan, S., and N. Arunachalam. 2016. "Strength of reinforced concrete beams partly curved in elevation." *Asian J. Res. Social Sci. Human.* 6 (11): 374–389. https://doi.org/10.5958/2249-7315.2016.01199.0.

Salonga, J., and P. Gauvreau. 2014. "Comparative study of the proportions, form, and efficiency of concrete arch bridges." *J. Bridge Eng.* 19 (3): 04013010. https://doi.org/10.1061/(ASCE)BE.1943-5592.0000537.

Shankar Nair, R. 1986. "Buckling and vibration of arches and tied arches." *J. Struct. Eng.* 112 (6): 1429–1440. https://doi.org/10.1061/(ASCE)0733-9445(1986)112:6(1429).

Wang, C. M., and C. Y. Wang. 2002. "Funicular shapes for submerged arches." *J. Struct. Eng.* 128 (2): 266–270. https://doi.org/10.1061/(ASCE)0733-9445(2002)128:2(266).